DensNet121 and Improved Hippopotamus Optimization Algorithm to Diagnosis Thyroid Nodules

Anwar Kadhem, Osama Majeed and Alaa Taima
College of Computer Science and Information Technology, Department of Computer Science, University of Al-Qadisiyah, 58001 Al-Diwaniyah, Iraq
cm.post23.1@qu.edu.iq, osama.m@qu.edu.iq, alaa.taima@qu.edu.iq

Keywords: Densnet121, Thyroid Nodules, Hippopotamus, Benign, Malignant, Artificial Intelligence.

Abstract: The diagnosis of thyroid nodules remains a challenge due to the limitations of conventional imaging techniques. This paper aims to improve the accuracy and efficiency of thyroid nodule diagnosis. The proposed densnet121-IHOA model is a good solution to the diagnostic accuracy problem. The proposed model consists of a densely connected network to extract features from ultrasound images. Several layers are added to perform the diagnosis process based on the features extracted by Densnet121. The optimal hyper-parameters for learning rate, batch size, dropout ratio, and number of neurons were found using an optimization algorithm. The improved hippopotamus algorithm (IHOA) is efficient in finding hyper-parameters. The IHOA algorithm is robust in exploring and exploiting solutions to find optimal values, and it does not require a large number of iterations. The dataset used in this paper is AUITD. The number of images used in the paper was 2,121, divided into 1,697 training images and 424 test images. The proposed model achieved an accuracy of 97.7%, precision of 96.3%, recall of 98%, and F1 score of 97.4%.

1 INTRODUCTION

The thyroid gland is one of the most important endocrine glands in humans [1]. Thyroid diseases have become common, as it is considered the second most common disease in the world [2]. Studies have confirmed an increase in the incidence of this disease [3],[4]. In a study conducted in Iraq at the Hussein Cancer center thyroid nodules ranked tenth with a rate of 2.7% of the incidence rate [5]. From this standpoint, early diagnosis is of utmost importance to control the development of the disease and treat it in its early stages and avoid the need for surgical removal of the gland [6]. Among the most important known methods used to diagnose nodules is ultrasound imaging. It is inexpensive and, most importantly, does not cause harm to the patient [7], [8], [9]. Ultrasound images are usually used to diagnose thyroid nodules by experts, and these traditional methods require a lot of effort and time, and sometimes the diagnosis may be inaccurate [10]. Recently, machine learning and deep learning have been widely used to help detect and diagnose thyroid nodules [11], [12]. Convolutional neural networks, especially pre-trained networks, are the leaders in this field, but they require tuning of hyper-parameters to achieve the desired result [13],[14]. To solve the problem of tuning hyper-parameters for transfer learning networks, optimization algorithms were used to perform this task and facilitate the work.

2 RELATED WORKS

In [15], Alghanimi et al. presented a new model ResNet50-pca based on feature selection technique using principal component analysis (PCA) and ResNet50. In order to reduce the dimensions of the dataset and maintain the highest degree of variance between classes in order to improve the classification process. The dataset used in this study is publicly available in (kaggle) under the name AUITD. 800 images were taken from it to conduct this study, 400 images for each class.

Kuma et al. proposed in [16] to classify thyroid nodules, which is mainly based on the (Resent50) model, which is one of the models trained on (ImageNet) data from the transfer learning model group. The dataset used to train the model consists of 1600 ultrasound images taken from a hospital in Algeria. The accuracy achieved by the model

reached 96.2% compared to the model called (AlexNat) which achieved 83.59%.

Alghanimi et al. proposed a diagnostic model in [17] using feature extraction techniques by (CNN) and transfer learning network (Resnet50) to classify thyroid nodules. The data used in this study were taken from AUITD which consists of 800 ultrasound images, 400 for benign category and 400 for malignant category. The CNN model achieved an accuracy of 91.25% while Resnet50 achieved an accuracy of 89.37%.

In [18] Wang et al. presented a different approach to diagnosing nodules using ultrasound. They proposed a new method for diagnosing thyroid cancer, using deep learning. The model was designed as a network that integrates the features extracted from the input ultrasound images and merges them into a single scan by using different views to improve the pattern recognition efficiency. The data used in this study was very large, which increased the reliability of the model's performance. The accuracy achieved in this study was 87.32%.

In [19] Nguyen et al. presented a multi-CNN model to solve the data imbalance problem fundamentally. Because multi-CNN analyzes images and extracts deeper features compared to a single CNN model. The dataset adopted in this study is TDID imbalanced. The achieved accuracy was 92.05%.

In [20] Pal et al. presented a study on designing a model for early detection of thyroid disease. The proposed model was built based on a database from the CUI repository and machine learning techniques. Three machine learning models were used in this study, namely (KNN, DT, MPL) nearest neighbors, decision tree and multilayer perceptron to predict the disease. The best performance was MPL, which achieved an accuracy of 95.73%.

In [21] Zhang et al. presented a diagnostic model for multi-class thyroid disease diagnosis. The model architecture consists of a novel multi-channel convolutional neural network. This proposed architecture integrates the extracted feature maps, which leads to an increase in diagnosis accuracy compared to the traditional CNN. The data used are CT images from GitHub. The achieved accuracy of the model was 90.9%.

In [22] Pavithra et al. presented a study on the diagnosis of thyroid tumors based on deep learning and ultrasound image data. The residual network (ResNet), which is one of the deep neural networks, was used. This study aimed to classify nodules into six groups according to the TI-RADS classification. The model achieved an accuracy of 83%.

In [23] Jopate et al. proposed a technique for selecting optimal and distinctive features using the AEHOA algorithm, an elephant herd optimization algorithm, and also eliminating the limitations related to overlearning. Due to the imbalance of the data, the SMOTE technique was used to balance the data. The features obtained by the elephant optimization algorithm were fed into a CNN network for prediction and classification of the data. The data were downloaded from the UCI ML repository and also modified to increase the classification accuracy. This method achieved an accuracy of 88.2%.

In [24] Kumar et al. proposed an advanced model based on differential evolution (DE) with butterfly optimization (BOA) and fuzzy c-means algorithm to improve the classification of thyroid disorder. The proposed model (DEBOA-FCM) was evaluated by several metrics, and the accuracy achieved by the model was 94.3%. It is worth mentioning that the data was well processed and modified to achieve high accuracy.

In [25] Ma et al. presented an effective diagnostic model by developing a convolutional neural network and a nature-derived optimization algorithm. The DensNet architecture was modified to build the model and the flower pollination algorithm was used to adjust the learning rate. The data used in this study were (SPECT image) consisting of three classes and were divided into training and testing data. The results achieved by the model were excellent compared to previous studies on the same database.

In [26] Sharma et al. presented new techniques for extracting thyroid features from medical images. The feature extraction was based on image transformer and Deit techniques. Six different techniques were used to reduce the dimensionality of the data in order to avoid oversampling and prevent overlearning. The FOX optimization algorithm was used to select the best features for the data. Two different types of databases were used, and the accuracy achieved was high.

In this research [27] Hemapriya et al. presented a model for diagnosing thyroid nodules. Initially, the pre-processing of the data was based on isolated forest with data normalization to detect outliers and eliminate noise. The feature extraction process is done by AlexNet improved by (CSA) algorithm to distinguish the most accurate patterns. Then (AGTO) was used with hybrid feature selection under the name (HAGTEO) to identify the important features, which leads to reducing the dimensions. Then, the data classification process is done by using GRU based on the extracted features. This method achieved an accuracy of 98%

3 METHODOLOGY

In this section, the dataset, preprocessing, and model architecture will be defined (Figure 1 shows the model architecture for thyroid nodules diagnosis). The proposed model is an effective method for diagnosis thyroid nodules. The proposed model (Densnet121-IHOA), consists of a densely connected convolutional network with 121 layers (DensNet121) and is one of the transfer learning techniques in addition to using the improved hippopotamus optimization algorithm (IHOA) to adjust the hyper-parameters.

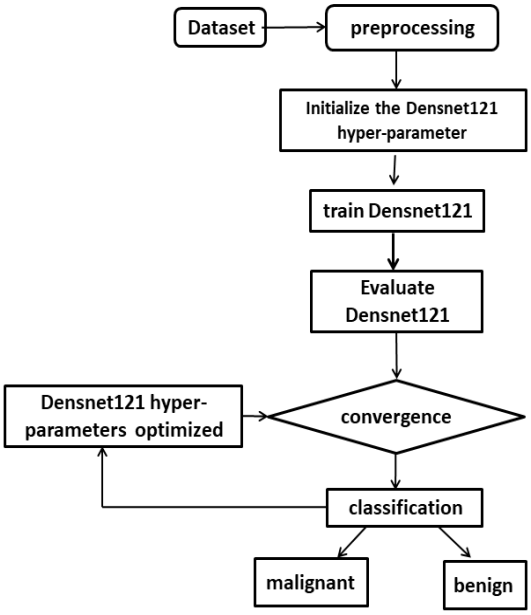

Figure 1: The proposed model.

3.1 Dataset

In this paper, we relied on the (AUITD) dataset from a hospital in Algeria. This data consists of ultrasound images of thyroid nodules. The dataset contains three categories, the benign category contains 1472 images, the malignant category contains 1895 images, and the normal or non-affected category contains 171 images. The dataset is divided into two files, training data and test data. The total number of available data that was downloaded is 2121 images, benign and malignant categories[28]. Figure 2 shows a sample of images of thyroid nodules in the two categories of malignant, benign.

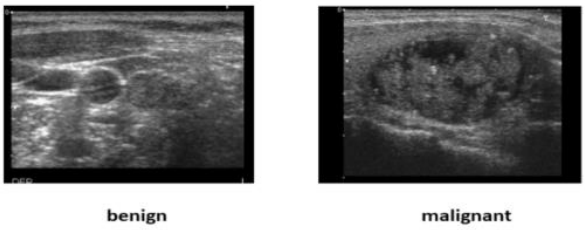

Figure 2: The sample malignant, benign.

3.2 Preprocessing

The data used in this paper have been processed to achieve real results. The processing process consisted of several stages.

1) At first, a specific cropping technique was applied to the image frame to get rid of only the dark frame and some details such as texts related to dimensions and device type, etc., if they remain, the model may consider them as a feature and learn them.
2) De-noise by applying the median filter. This filter is considered the best for De-noise while preserving the borders and shapes within the image.
3) At this stage, the images were resized using the scaling technique to dimensions 128x128 so that all images would be of equal dimensions and also to achieve compatibility between the model and the data.
4) At this final stage, the images were normalized to match the data with the model inputs.

3.3 Proposed Model

The proposed paper aims to achieve the highest accuracy in diagnosing thyroid nodules. The transfer learning technique (DensNet121) was primarily used to extract features, and custom layers were added to perform the diagnosis process. Meta-heuristic algorithms were used to fine-tune the hyper-parameters of the proposed model. The hyper-parameters that were optimized include the learning rate, batch size, number of neurons, and dropout rate. The Improved hippopotamus Algorithm (IHOA), an improved version of the original hippopotamus algorithm was used. A comprehensive overview of the hippopotamus algorithm and the improvements made to it to increase its effectiveness with the proposed model is presented.

3.3.1 Densnet

In this paper, densnet121 was used. It which consists of four blocks in the following order (6,12,24,16). Pre-trained networks or so-called learning transfer techniques have solved many issues related to medical image classification [29]. One of the most powerful learning transfer techniques in medical image classification is densely connected convolutional neural networks (DensNet) . This technique addressed one of the most important issues related to increasing the depth of the network, which is the issue of gradient or feature disappearance. In a DensNet network, each layer is connected to all the layers that precede it, and this is where its strength lies, as features do not disappear or are dropped, but are passed on to the next layer [30]. Figure 3 shows the structure of a DensNet121 and how its layers are connected to each other.

3.3.2 Hippopotamus Optimization Algorithm

The hippopotamus algorithm was proposed in 2024 by Amiri. This algorithm relies on the unique behaviors of hippopotamuses to find solutions to optimization problems. The unique behaviors of hippopotamuses, such as their constant changing of positions in rivers and ponds, their defense against predators, and the process of escaping from predator attacks, are considered. These three behaviors were converted into mathematical equations by the algorithm's proposer [31] .

HO population initialization phase Generating random initial solutions. A random initial solution vector is generated based on the following (1):

$$x_i: x_{ij} = lb_j + r.\left(ub_j - lb_j\right) \quad (1)$$
$$i = 1,2,\dots,N, j = 1,2,\dots,m \ .$$

Where Xi represents the positions, lb and ub represents lower and upper bounds, r random number, jth decision variable , N denotes the population size, M represents the number of decision variables.

$$X = \begin{bmatrix} \chi_1 \\ \vdots \\ \chi i \\ \vdots \\ \chi N \end{bmatrix}_{N\times m} = \begin{bmatrix} x_{1,1} & \cdots & v_{1,y} & \cdots & x_{1,m} \\ \vdots & \ddots & \vdots & \iddots & \vdots \\ x_{i,1} & \cdots & x_{i,y} & \cdots & x_{i,m} \\ \vdots & \iddots & \vdots & \ddots & \vdots \\ x_{N,1} & \cdots & x_{N,y} & \cdots & x_{N,m} \end{bmatrix}_{N\times m} \quad (2)$$

Stage 1. Hippopotamuses change their locations in water bodies and rivers (exploration). hippopotamus groups consist of adult males, adult female hippopotamus and young hippopotamus. The group has a leader called the dominant male who is determined based on the value of the objective function. One of the behaviors of hippopotamus is that they are close to each other. The dominant hippos protect the herd and the area of the group. Many females are placed around the male hippopotamus. When the male hippopotamus reach maturity, they are expelled by the leader of the herd (the dominant). The males that have been expelled from the herd either attract females or enter into dominance competitions with the dominant hippopotamus in the herd to prove their dominance. The mathematical representation of this stage is done through (3)

$$x_i^{Mhippo}: x_{ij}^{Mhippo} = x_{ij} + y_1.\left(D_{hippo} - I_{1x_{ij}}\right). \quad (3)$$

$X_i^{\boldsymbol{M}hippo}$ represents male hippopotamus sites.

D^{hippo} represents the dominant hippopotamus .

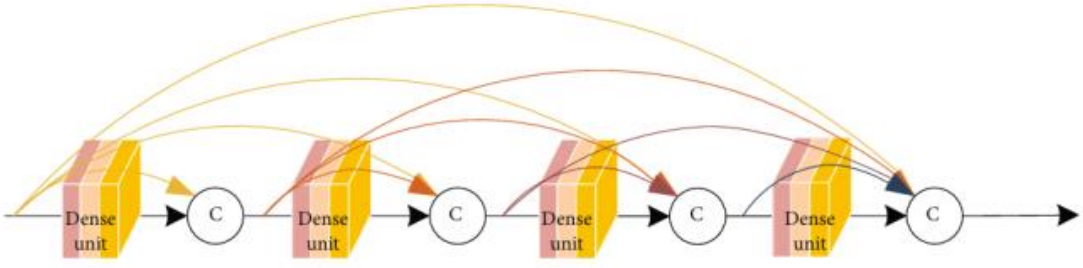

Figure 3: Structure of a DensNet121.

$$\mathcal{K} = \begin{cases} I_2 \times \vec{r}_1 + (\sim \varrho_1) \\ 2 \times \vec{r}_2 - 1 \\ \vec{r}_3 \\ I_1 \times \vec{r}_4 + (\sim \varrho_2) \\ r_5 \end{cases} . \quad (4)$$

I_1,I_2 is an integer between 1 and 2, $r_{1,2,3,4}$ is random vector in range 0 and 1 , r_5 random number ϱ_2, ϱ_1 integer random number 0 or 1

$$T = exp\left(-\frac{t}{T}\right). \quad (5)$$

$$x_i^{\mathbf{FB}\text{hippo}} : x_{ij}^{\mathbf{FB}\text{hippo}} = \begin{cases} X_{ij} + h_1.\left(D_{hippo} - I_2 MG_i\right) T > 0.6 \\ \Xi \qquad\qquad\qquad\qquad \text{else} \end{cases} . \quad (6)$$

Where in (6) - $x_1^{\mathbf{FB}\text{hippo}}$ represents the position of a female hippopotamus or an immature hippopotamus.

$$\Xi = \begin{cases} x_{ij} + h_2.\left(MG_i - D_{hippo}\right) r_6 > 0.5 \\ lb + r_7.\left(ub_i - lb_j\right) \quad else \end{cases} . \quad (7)$$

$$x_i = \begin{cases} x_i^{Mhippo} F_i^{Mhippo} < F_i \\ x_i \qquad\qquad\qquad else \end{cases} . \quad (8)$$

$$x_i = \begin{cases} x_i^{\boldsymbol{FB}ippo} F_i^{\boldsymbol{FB}ippo} < F_i \\ x_i \qquad\qquad\qquad else \end{cases} . \quad (9)$$

Stage 2. In this stage, the process of defense against predators (exploration) takes place. One of the most important reasons for hippos to live in groups is for their safety. The presence of hippopotamus in groups is a reason to prevent predators from attacking them or approaching their geographical area. however, immature hippopotamus may tend to separate from the herd and thus become easy targets for predators. Also, sick or old hippopotamus may meet their fate at the hands of predators. In this case, the hippopotamus is switched to defense mode by heading towards the predator, opening its large jaws, making sounds to scare the predator, and sometimes approaching the predator to encourage it to move away. In (10), the predator is placed in the search space.

$$Predator: Predator_j = lb_j + \vec{r_8}.\left(ub_j - lb_j\right), \quad (10)$$
$$j = 1, .., m.$$

$$\vec{D} = \left|Predator_j - x_{ij}\right|. \quad (11)$$

where D is the distance between the hippopotamus and the prey.

When the predator approaches the hippopotamus, the latter adopts a defensive behavior based on $F_{predator}$ to protect itself from the predator's attack. If F_i is greater than $F_{predator}$, this means that the predator is close to the hippopotamus' territory. In this case, the hippopotamus moves towards the predator to make it move away from the borders of the territory. If F_i is less than $F_{predator,}$ this means that the predator is within the hippopotamus' territory and is very close to it. In this case, the hippopotamus moves towards the predator to scare it away, but its movement is limited because intruder is very close to the hippopotamus (12).

Where in (12) - x_i^{HippoR} is the position of the hippopotamus facing the predator. RL is a random vector generated by the Lévy algorithm distribution used for sudden changes in predator positions during an attack. This process is done by (13). Where in (13) - v ,w is random number.

$$\mathcal{L}_{evy}(\vartheta) = 0.05 \times \frac{w \times \sigma_w}{|v|^{\frac{1}{\vartheta}}} \quad (13)$$

$$\sigma_w = \left[\frac{\Gamma(1+\vartheta)\sin\left(\frac{\pi\vartheta}{2}\right)}{\Gamma\left(\frac{(1+\vartheta)}{2}\right)\vartheta 2^{\frac{(\vartheta-1)}{2}}}\right]^{\frac{1}{\vartheta}} . \quad (14)$$

$$\chi_i = \begin{cases} \chi_i^{\mathcal{H}ippoR} \mathcal{F}_i^{\mathcal{H}ippoR} < \mathcal{F}_i \\ \chi_i \mathcal{F}_i^{\mathcal{H}ippoR} \geq \mathcal{F}_i \end{cases} \quad (15)$$

If it is hunted by a predator, it replaces the position of one of the herd members, otherwise it will return to its previous position.

$$\chi_i^{\mathcal{H}ippoR} : x_{ij}^{\mathcal{H}ippoR} = \begin{cases} \vec{RL} \oplus \mathcal{P}redator_j + \left(\frac{\ell}{(-\mathcal{K}\cos(2\pi\mathcal{g}))}\right).\left(\frac{1}{\vec{\mathcal{D}}}\right)\mathcal{F}_{\mathcal{P}redator_j} < \mathcal{F}_i \\ \vec{RL} \oplus \mathcal{P}redator_j + \left(\frac{\ell}{(-\mathcal{K}\cos(2\pi\mathcal{g}))}\right).\left(\frac{1}{2\times\vec{\mathcal{D}}+\vec{r}_9.}\right)\mathcal{F}_{\mathcal{P}redator_j} \geq \mathcal{F}_i \end{cases} \quad (12)$$

Stage 3. Escape (Exploitation). A hippopotamus behavior occurs when it encounters a predator that it is unable to confront defensively. The hippopotamus flees to a pond near its current location. New locations (ponds) are generated randomly using (17). This behavior protects the hippopotamus from predation (predators avoid entering the water). If the new location is more favorable than the current location (based on the cost function), the hippopotamuses location is updated using (19).

$$lb_j^{local} = \frac{lb_j}{t}, ub_j^{local} = \frac{ub_j}{t}, t = 1, 2, \ldots, T. \quad (16)$$

Where lb, ub It indicates lower and upper bounds t current iteration.

$$x_{ij}^{HippoE} = x_{ij} + r_{10,\cdot}\left(lb_j^{local} + \vartheta_{1,\cdot}\left(ub_j^{local} - lb_j^{local}\right)\right) \quad (17)$$

Where $X_{i,j}^{HippoE}$ New site.

$$\vartheta = \begin{cases} 2 \times \overrightarrow{r}_{11} - 1 \\ r_{12} \\ r_{13} \end{cases}. \quad (18)$$

Where s random numbers .

$$\chi_i = \begin{cases} \chi_i^{\mathcal{H}ippoE} & \mathcal{F}_i^{\mathcal{H}ippoE} < \mathcal{F}_i \\ \chi_i & \mathcal{F}_i^{\mathcal{H}ippoE} \geq \mathcal{F}_i \end{cases}. \quad (19)$$

F represent of the cost function.

3.3.3 Improved Hippopotamus Optimization Algorithm

The Improved process was done on the third stage of the hippopotamus algorithm. The Improved were made to the algorithm to improve the exploitation of the solutions discovered so far from the first and second stages instead of discovering new solutions. The process of improving the discovered solutions depends entirely on the best solution discovered so far. This technique has been applied in many optimization algorithms such as the PSO algorithm[32]. To gradually reduce randomness and increase the exploitation power in the final stages, the exponential decay technique was relied upon. Equations (16) and (17) in the Hippopotamus algorithm were replaced with the following new (20) and (21).

$$E(t) = e^{-\frac{t}{T}}. \quad (20)$$

t current iteration and T max iteration

$$x_{i,j}^{Hippo} = x_{i,j} + E(t)\left(x_{i,j}^{best} - x_{i,j}\right) + D. \quad (21)$$

where $D = (\text{rendom number})(0.01)$

Added a small noise D to improve local exploitation and avoid falling into local solutions.

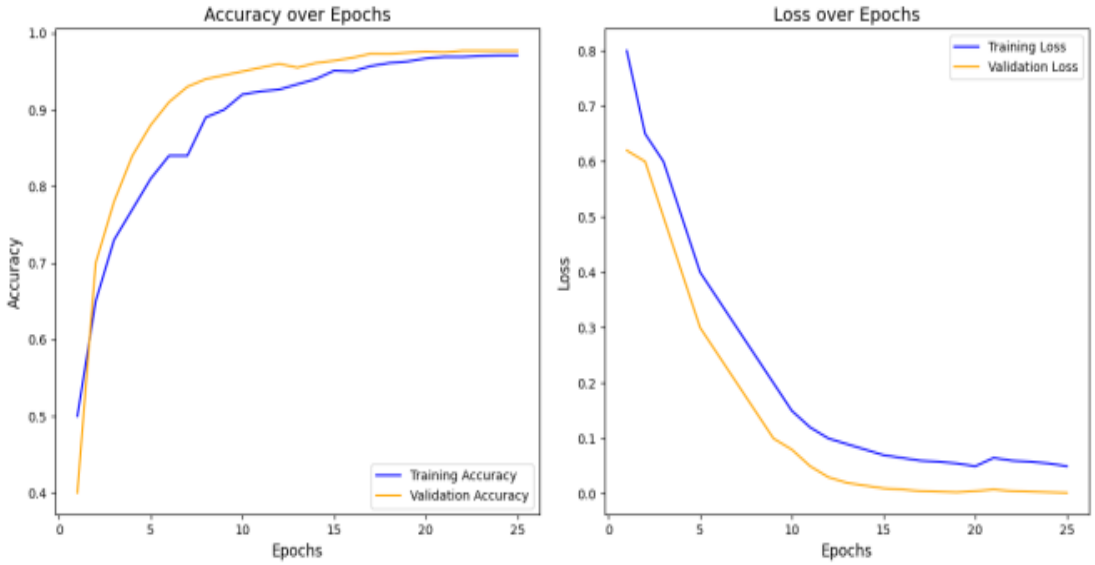

Figure 4: The performance proposed model.

4 EXPERIMENTAL RESULTS

In this section will show the results obtained from training the DensNet121-IHOA model on the AUITD dataset. The model code was written using python 3.11.0 with pycharm environment. The model was run on an HP laptop with Ryzen 7 processor, G32 RAM and Vega 4G graphics processor.

The AUITD dataset contains two classes, malignant and benign. The dataset is divided into 0.07% training, 0.01% validation and 0.02% testing to train and test the proposed model. Table 1 shows the training results before and after improved optimization algorithm. Figure 4 shows the accuracy curve and loss curve of the proposed model.

The training results in Table 1: showed the performance of the DensNet121-IHOA model, which achieved an accuracy of 97.7% compared to the Densnet121-HOA model before the hippopotamus Improved algorithm, where the achieved accuracy was 97.02%.

As for training the Densnet121 model without using the optimization algorithm (HOA) and (I-HOA), it achieved an accuracy of 96%, and this performance is low compared to the Densnet121-IHOA model. The reason for the low accuracy of DensNet121 is the collapse of the hyper-parameters tuning accurately.

The training results confirmed that incorporating optimization algorithms significantly enhances the model's accuracy, in addition to fine-tuning the model's hyper-parameters. As for the results obtained from the DensNet121-IHOA model, the accuracy increased by 0.069% compared to the Densnet121-HOA model.

Table 1: the training results.

model	Performance			
	Acc	Prec	Rec	F1
Densnet121-HOA	97.1%	97.3%	94.6	96.03
Densnet121-IHOA	97.7%	96.3	98.7	97.4

Comparison of the proposed model with other techniques based on the results. The proposed model achieved high accuracy with low loss ratio. The Densnet technique used for feature extraction was robust compared to other techniques. The Dense connections between the layers of the Densnet network ensured smooth flow of information and no feature loss across layers. Table 2 shows the results of the comparison with other techniques.

Table 2: Comparison of the proposed model with other techniques.

Authors	AUITD Dataset	Accuracy
[15] Alghanimi et al.	800 images	89.54%
[16] Kuma et al.	1600 images	96.20%
[17] Alghanimi et al.	800 images	91.25%
Proposed model	2121 images	97.7%

Figure 5 shows the confusion matrix for the test data. The reason for some misdiagnosis of images is due to the use of the sigmoid function to perform the classification process.

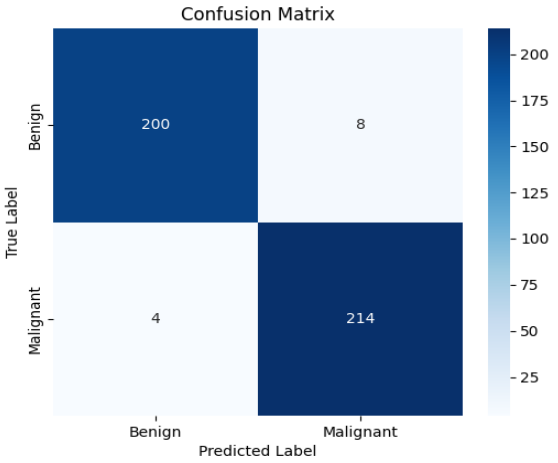

Figure 5: The confusion matrix of proposed model.

5 CONCLUSIONS

This paper presented a high-accuracy diagnostic model for thyroid nodules. Transfer learning was used in this paper to solve the problem of data unavailability. To address the problem of adjusting hyperparameters in transfer learning models, the (I-HOA) algorithm was used for tuning. Diagnosis by computer models has a great impact on the early recognition of diseases. Computer models provide immediate solutions and help in making early decisions to detect diseases and reduce their impact and spread in society. Expected future work includes collecting more data from specialized medical centers to improve the performance of the model. We hope to use the model in hospitals and centers specialized in detecting and treating tumors, as well as cooperate with specialists to develop the model to be more reliable in decision-making. The number of images used in the paper was 2,121, divided into 1,697 training images and 424 test images. The proposed

model achieved an accuracy of 97.7%, precision of 96.3%, recall of 98%, and F1 score of 97.4%.

REFERENCES

[1] N. Q. Tran, B. H. Le, C. K. Hoang, H. T. Nguyen, and T. T. Thai, "Prevalence of Thyroid Nodules and Associated Clinical Characteristics: Findings from a Large Sample of People Undergoing Health Checkups at a University Hospital in Vietnam," Risk Manag. Healthc. Policy, vol. 16, pp. 899–907, 2023, doi: 10.2147/RMHP.S410964.

[2] H. Yu et al., "Intelligent diagnosis algorithm for thyroid nodules based on deep learning and statistical features," Biomed. Signal Process. Control, vol. 78, p. 103924, 2022, doi: 10.1016/j.bspc.2022.103924.

[3] X. Wu, B. L. Li, C. J. Zheng, and X. D. He, "Predictive factors for central lymph node metastases in papillary thyroid microcarcinoma," World J. Clin. Cases, vol. 8, no. 8, pp. 1350–1360, 2020, doi: 10.12998/WJCC.V8.I8.1350.

[4] L. Enewold et al., "Rising thyroid cancer incidence in the United States by demographic and tumor characteristics, 1980-2005," Cancer Epidemiol. Biomarkers Prev., vol. 18, no. 3, pp. 784–791, 2009, doi: 10.1158/1055-9965.EPI-08-0960.

[5] A. Mjali and B. Najeh Hasan Al Baroodi, "Some Facts About Cancers in Karbala province of Iraq, 2012-2020," Asian Pacific J. Cancer Care, vol. 5, no. 2, pp. 67–69, 2020, doi: 10.31557/apjcc.2020.5.2.67-69.

[6] K. Kourou, T. P. Exarchos, K. P. Exarchos, M. V. Karamouzis, and D. I. Fotiadis, "Machine learning applications in cancer prognosis and prediction," Comput. Struct. Biotechnol. J., vol. 13, pp. 8–17, 2015, doi: 10.1016/j.csbj.2014.11.005.

[7] J. Xia et al., "Ultrasound-based differentiation of malignant and benign thyroid Nodules: An extreme learning machine approach," Comput. Methods Programs Biomed., vol. 147, pp. 37–49, 2017.doi: 10.1016/j.cmpb.2017.06.005

[8] S. Y. Ko et al., "Deep convolutional neural network for the diagnosis of thyroid nodules on ultrasound," Head Neck, vol. 41, no. 4, pp. 885–891, 2019.doi: 10.1016/j.media.2020.101665.

[9] J. Chen, H. You, and K. Li, "A review of thyroid gland segmentation and thyroid nodule segmentation methods for medical ultrasound images," Comput. Methods Programs Biomed., vol. 185, p. 105329, 2020.doi: 10.1016/j.cmpb.2020.105329.

[10] M. D. Russell and L. A. Orloff, "Ultrasonography of the thyroid, parathyroids, and beyond," HNO, vol. 70, no. 5, pp. 333–344, 2022.doi: 10.1007/s00106-022-01162-0.

[11] S. Razia and M. R. N. Rao, "Machine learning techniques for thyroid disease diagnosis-a review," Indian J Sci Technol, vol. 9, no. 28, pp. 1–9, 2016.doi: 10.17485/ijst/2016/v9i28/93705

[12] G. Zhang and V. L. Berardi, "An investigation of neural networks in thyroid function diagnosis," Health Care Manag. Sci., vol. 1, pp. 29–37, 1998.doi: 10.1023/A:1019078131698.

[13] M. A. K. Raiaan et al., "A systematic review of hyperparameter optimization techniques in Convolutional Neural Networks," Decis. Anal. J., vol. 11, p. 100470, 2024, doi: 10.1016/j.dajour.2024.100470.

[14] M. Iman, H. R. Arabnia, and K. Rasheed, "A review of deep transfer learning and recent advancements," Technologies, vol. 11, no. 2, p. 40, 2023.doi: 10.3390/technologies11020040.

[15] G. B. Alghanimi, H. Aljobouri, K. A. Alshimmari, and R. Massoud, "Effective Feature Selection on Transfer Deep Learning Algorithm for Thyroid Nodules Ultrasound Detection," Al-Nahrain J. Eng. Sci., vol. 27, no. 4, pp. 396–401, 2024. 10.29194/NJES.27040396.

[16] J. Kumar, S. Narayan Panda, and D. Dayal, "Utilizing Deep Learning Models for the Classification of Thyroid Nodules in Ultrasound Images," pp. 18–31, 2023, [Online]. Available: www.theijes.com.doi: 10.9790/1813-12111831.

[17] G. B. Alghanimi, H. K. Aljobouri, and K. A. Al-shimmari, "CNN and ResNet50 Model Design for Improved Ultrasound Thyroid Nodules Detection," in 2024 ASU International Conference in Emerging Technologies for Sustainability and Intelligent Systems (ICETSIS), IEEE, 2024, pp. 1000–1004.doi: 10.1109/ICETSIS61505.2024.10459588.

[18] L. Wang, L. Zhang, M. Zhu, X. Qi, and Z. Yi, "Automatic diagnosis for thyroid nodules in ultrasound images by deep neural networks," Med. Image Anal., vol. 61, p. 101665, 2020.doi: 10.1016/j.media.2020.101665.

[19] D. T. Nguyen, J. K. Kang, T. D. Pham, G. Batchuluun, and K. R. Park, "Ultrasound image-based diagnosis of malignant thyroid nodule using artificial intelligence," Sensors, vol. 20, no. 7, p. 1822, 2020.doi: 10.3390/s20071822.

[20] M. Pal, S. Parija, and G. Panda, "Enhanced prediction of thyroid disease using machine learning method," in 2022 IEEE VLSI Device Circuit and System (VLSI DCS), IEEE, 2022, pp. 199–204.doi: 10.1109/VLSIDCS53788.2022.9811472.

[21] X. Zhang, V. C. S. Lee, J. Rong, J. C. Lee, J. Song, and F. Liu, "A multi-channel deep convolutional neural network for multi-classifying thyroid diseases," Comput. Biol. Med., vol. 148, p. 105961, 2022, doi: 10.1016/j.compbiomed.2022.105961.

[22] S. Pavithra, G. Yamuna, and R. Arunkumar, "Deep learning method for classifying thyroid nodules using ultrasound images," in 2022 International Conference on Smart Technologies and Systems for Next Generation Computing (ICSTSN), IEEE, 2022, pp. 1–6.doi: 10.1109/ICSTSN53084.2022.9761364.

[23] R. Jopate, P. K. Pareek, D. M. G. Jyothi, and A. S. Z. J. Al Hasani, "Prediction of Thyroid Classes Using Feature Selection of AEHOA Based CNN Model for Healthy Lifestyle," Baghdad Sci. J., vol. 21, no. 5 SI, pp. 1786–1797, 2024, doi: 10.21123/bsj.2024.10547.

[24] S. J. K. Kumar, P. Parthasarathi, M. Masud, J. F. Al-Amri, and M. Abouhawwash, "Butterfly Optimized Feature Selection with Fuzzy C-Means Classifier for Thyroid Prediction.," Intell. Autom. Soft Comput., vol. 35, no. 3, 2023.doi: 10.32604/iasc.2023.030335.

[25] L. Ma, C. Ma, Y. Liu, and X. Wang, “Thyroid diagnosis from SPECT images using convolutional neural network with optimization,” Comput. Intell. Neurosci., vol. 2019, no. 1, p. 6212759, 2019.doi: 10.1155/2019/6212759.

[26] R. Sharma et al., “Comparative performance analysis of binary variants of FOX optimization algorithm with half-quadratic ensemble ranking method for thyroid cancer detection,” Sci. Rep., vol. 13, no. 1, p. 19598, 2023.doi: 10.1038/s41598-023-46865-8.

[27] K. Hemapriya and K. Valarmathi, “Innovative Framework for Thyroid Disease Detection by Leveraging Hybrid AGTEO Feature Selection and GRU Classification Model,” Int. Res. J. Multidiscip. Technovation, vol. 6, no. 3, pp. 112–127, 2024.doi: 10.54392/irjmt2439.

[28] A. Maroua, “Algeria Ultrasound Images Thyroid Dataset (AUITD).” [Online]. Available: https://www.kaggle.com/datasets/azouzmaroua/algeria-ultrasound-images-thyroid-dataset-auitd/data

[29] G. Huang, Z. Liu, L. Van Der Maaten, and K. Q. Weinberger, “Densely connected convolutional networks,” in Proceedings of the IEEE conference on computer vision and pattern recognition, 2017, pp. 4700–4708.dio: unavailable

[30] T. Zhou, X. Ye, H. Lu, X. Zheng, S. Qiu, and Y. Liu, “Dense convolutional network and its application in medical image analysis,” Biomed Res. Int., vol. 2022, no. 1, p. 2384830, 2022.doi: 10.1155/2022/2384830.

[31] M. H. Amiri, N. Mehrabi Hashjin, M. Montazeri, S. Mirjalili, and N. Khodadadi, “Hippopotamus optimization algorithm: a novel nature-inspired optimization algorithm,” Sci. Rep., vol. 14, no. 1, p. 5032, 2024.doi: 10.1038/s41598-024-54910-3.

[32] M. Jain, V. Saihjpal, N. Singh, and S. B. Singh, “An overview of variants and advancements of PSO algorithm,” Appl. Sci., vol. 12, no. 17, p. 8392, 2022.doi: 10.3390/app12178392.